

Supporting Information for

***In situ* tracing of atom migration in Pt/NiPt hollow spheres during catalysis of CO oxidation[†]**

Jialong Liu,^{a,b} Wei Liu,^{a,c} Qian Sun,^{a,d} Shouguo Wang,^{*b} Kai Sun,^{*c} Johannes Schwank^d and Rongming Wang^{*a}

^a Department of Physics, Beijing University of Aeronautics and Astronautics, Beijing 100191, P. R. China, E-mail: rmwang@buaa.edu.cn

^b State Key Laboratory of Magnetism, Institute of Physics, Chinese Academy of Sciences, Beijing 100190, P. R. China, E-mail: sgwang@iphy.ac.cn

^c Department of Materials Science & Engineering, University of Michigan, Ann Arbor, MI 48109 USA, Email: kaisun@umich.edu

^d Department of Chemical Engineering, University of Michigan, Ann Arbor, MI 48109 USA

I. Experimental Section

1. Synthesis

NaBH₄, K₂PtCl₆, NiCl₂ • 6H₂O and poly-vinylpyrrolidone (PVP) were purchased from Chinese reagent companies. All reagents were analytic grade and used without further purification. The solid NiPt spheres, hollow NiPt alloy spheres and hollow NiPt/Pt spheres were synthesized following previously described method.¹ For synthesis of solid NiPt spheres, NiCl₂ • 6H₂O (34 mg) and PVP (Mw=30000, 100 mg) were dissolved in 43 ml deionized water. Then the suspension was sonicated for 15 min and sequentially purged with N₂ for 15 min. A freshly prepared solution of NaBH₄ (10 mg in 20 ml of deionized water) was then added dropwise with magnetic stirring. After addition of NaBH₄ and as-prepared colloidal suspension turned black, immediately K₂PtCl₆ (20 ml 6mM) was added dropwise. For NiPt alloy hollow spheres and Pt/NiPt hollow spheres, K₂PtCl₆ of 20ml 6mM and 20ml 12mM were used respectively with NiCl₂ • 6H₂O of 17 mg while keeping other conditions unchanged. After 60 min, the product was collected by centrifugation and washed several times with H₂O and ethanol sequentially to remove the residual nonionic surfactant.

2. Structure Characterization

The FTIR spectra (2300-1800 cm⁻¹) of CO adsorption were recorded using a Bruker Tensor 27 spectrometer and diffuse reflectance infrared Fourier transform spectroscopy (DRIFTS) cell. Pt/NiPt samples (10 mg) pretreated in a 50% H₂-N₂ gas mixture at 350K for 1 hour and cooled down to room temperature were mixed with 90 mg KBr and pressed as tablet for the test cell.

The spectra were collected from 305 K to 390 K with a resolution of 4 cm⁻¹. For CO adsorption, a gas mixture of 1% CO (99.5% pure, Al tank) and 99% N₂ (99.999% pure) at a flow rate of 30 ml/min was inlet for 1h at each temperature. Then the cell was pumped to 1*10⁻⁵ mbars to remove the gaseous CO species and collect the spectra. For CO oxidation, a gas mixture of 1% CO (99.5% pure, Al tank), 1% O₂ (99.999% pure) and 98% N₂ (99.999% pure) at a total flow rate of 30 ml/min was inlet for 1h at each temperature. Then the cell was pumped to 1*10⁻⁵ mbars to remove the gaseous CO species and collect the spectra. The gases were introduced using carefully calibrated mass flow controllers. The time dependent spectra were collected at 390 K. Firstly, 1% CO was continuously input until a steady state was reached when CO was adsorbed on the sample surface with around saturation coverage. Then the chamber was pumped and the spectra were collected every one minute. The details of DRIFTS experiments can be found elsewhere.²

High angular annular dark field scanning transmission electron microscopy (HAADF-STEM) was carried out to investigate the morphologies and structures using a JEOL 2100F analytical microscope. A STEM probe corrector (CEOS GmbH probe correction) was utilized to acquire a spatial resolution around 1Å. To enable the direct observation of atoms distribution, the collect angle for HAADF imaging was set to be around 50 mrad. The specimens for the TEM studies were obtained by dispersion of the as-prepared products in ethanol and then a drop of the suspension was placed on a carbon coated copper grid and dried in air.

II. Supplementary Data

With increasing Pt/Ni ratio (referred as Pt/Ni), NiPt solid spheres were transformed into NiPt hollow spheres, and finally into Pt/NiPt hollow spheres. The ratio of Pt/Ni=1 resulted in solid NiPt spheres (Fig. S1a and d) with a Ni-rich core and an ultra-thin NiPt alloyed shell. For Pt/Ni ratio up to 2, large-scale NiPt hollow spheres were obtained, (Fig. S1b and e), where NiPt alloyed shell and hollow structure were shown by the white clean shell and black interior, respectively. At last, large-scale talented Pt/NiPt spheres (Fig. S1c and f) were acquired using excessive Pt precursor with Pt/Ni=4.

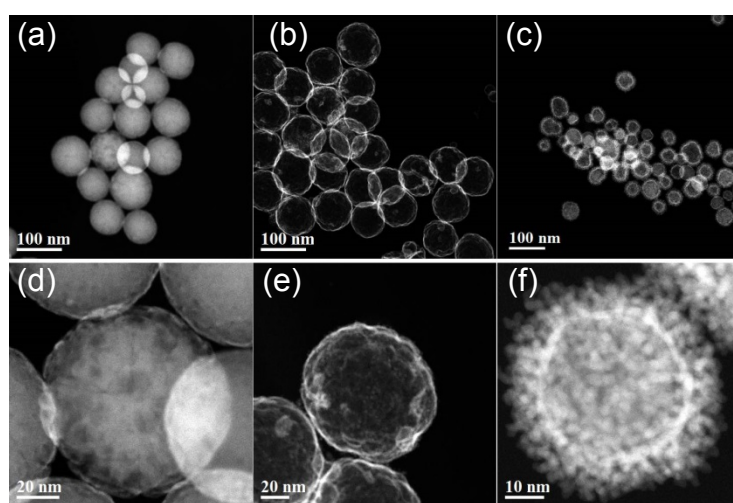


Figure S1: Dark-field STEM images of mono-dispersed samples. (a and d) NiPt solid spheres with a Ni-rich core; (b and e) NiPt alloyed spheres with a hollow interior and a thin shell (2-3 nm). (c and f) Pt/NiPt hollow spheres with a layer of Pt adsorbed on NiPt hollow spheres.

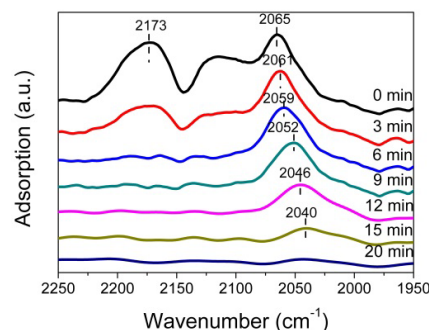


Figure S2: Time dependent DRIFTS of CO adsorption on Pt/NiPt at 390 K. The CO input was stopped and it started to pump until the peak at around 2060 cm^{-1} was disappeared. The peak at 2173 cm^{-1} that was disappeared after 6 minutes pumping was attributed to gaseous CO.

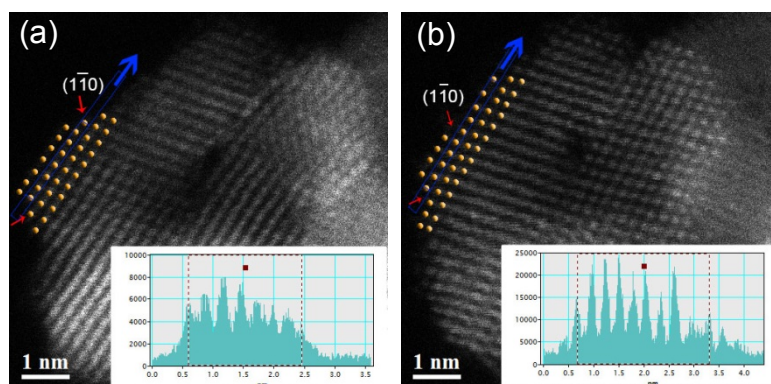


Figure S3: Planar atomic columns of external four Pt layers (a) before and (b) after the catalysis of CO oxidation in Region A. Insets were two lines scans of the intensity of HAADF signal along the directions of blue arrows.

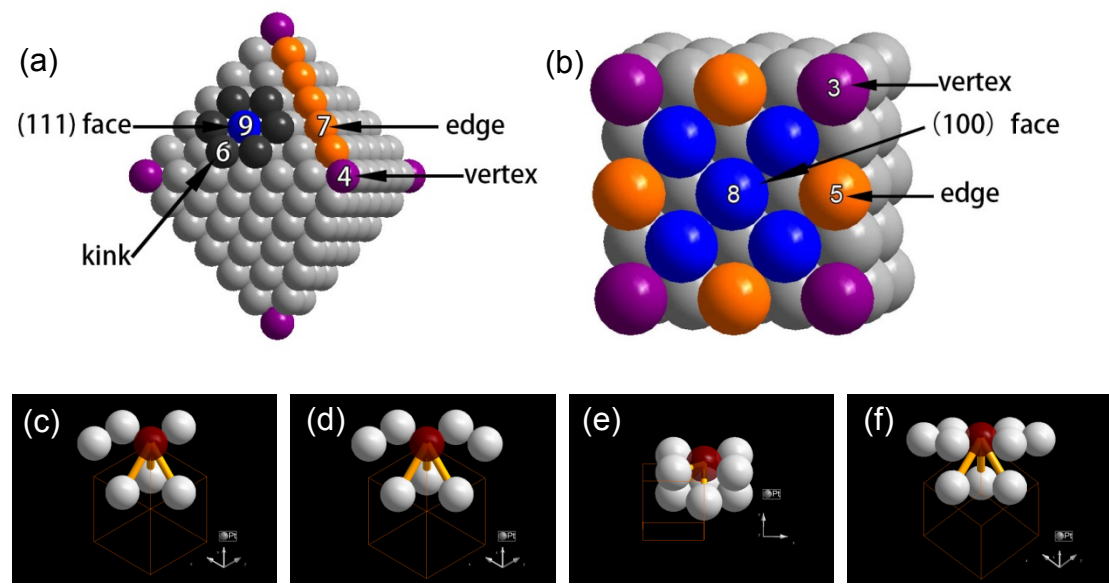


Figure S4: Models of (a) octahedral and (b) cubic nanocrystals showing different types of surface atomic sites and their coordination numbers. Surface atom models with coordination numbers of 6, 7, 8 and 9 from (c) to (f) correspond to atom located at kink site, step site, (100) terrace and (111) terrace.^{3,4}

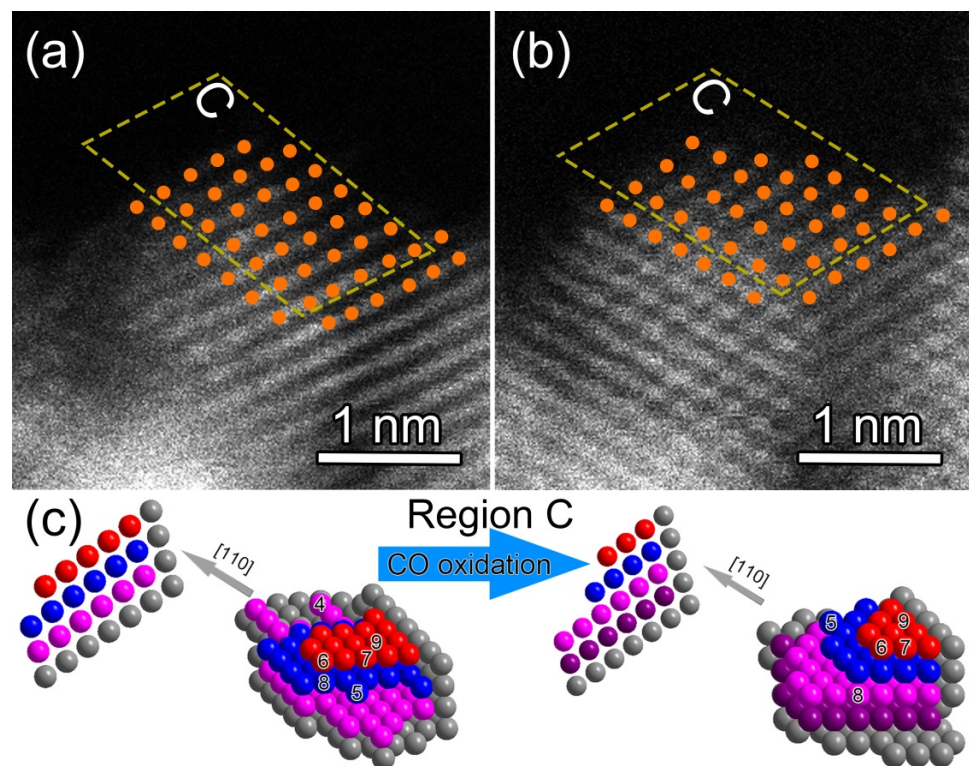


Figure S5: HAADF-STEM images of Pt atom migration during catalysis of CO oxidation. (a) As-prepared samples; (b) after catalytic process. 3D reconstructed atomic models and projections during catalytic process of Region C, where red, blue and pink balls for different layer and gray balls for substrate, respectively. The number labeled on the ball is the coordination number at various sites.

Table S1: Atoms with different coordination numbers measured in the 3D reconstructed structures of Region A, B in Fig. 3 and Region C in Fig. S5. The differences reveal atomic migration during catalysis of CO oxidation.

coordination number	Region A			Region B			Region C		
	before	after	difference	before	after	difference	before	after	difference
12	34	31	-3	31	32	1	28	37	9
11	10	7	-3	6	5	-1	7	7	0
10	11	8	-3	6	3	-3	6	5	-1
9	7	18	11	18	22	4	15	8	-7
8	21	13	-8	10	8	-2	9	14	5
7	9	17	8	12	16	4	14	10	-4
6	12	9	-3	11	11	0	9	11	2
5	10	8	-2	7	5	-2	4	3	-1
4	4	3	-1	3	2	-1	2	0	-2
3	0	0	0	0	0	0	0	0	0
2	0	0	0	0	0	0	0	0	0
1	0	0	0	0	0	0	0	0	0

References

- Q. Sun, Z. Ren, R. Wang, N. Wang and X. Cao, *Journal of Materials Chemistry*, 2011, **21**, 1925-1930.
- R. Wang, H. He, J. N. Wang, L. C. Liu and H. X. Dai, *Catal Today*, 2013, **201**, 68-78.
- R. K. Brandt, R. S. Sorbello and R. G. Greenler, *Surface Science*, 1992, **271**, 605-615.
- M. I. Monine, L. M. Pismen and R. Imbihl, *J Chem Phys*, 2004, **121**, 11332-11344.